Sulfated galactan derivatives from *Gracilaria fisheri* suppress the proliferation of MCF-7 breast cancer cells by inducing cell cycle arrest

JENJIRALAI PHANPHAK[1], SOMSUDA SOMINTARA[1], WARAPORN SAKAEW[1], THANYAPORN SENARAI[1], JOSÉ KOVENSKY[2], KANOKPAN WONGPRASERT[3] and TAWUT RUDTANATIP[1]

[1]Electron Microscopy Unit, Department of Anatomy, Faculty of Medicine, Khon Kaen University, Khon Kaen 40002, Thailand; [2]Laboratory of Glycochemistry and Agroresources UR 7378, Picardie Institute of Chemistry FR 3085, University of Picardie Jules Verne, 80000 Amiens, France; [3]Department of Anatomy, Faculty of Science, Mahidol University, Bangkok 10400, Thailand

Received March 13, 2025; Accepted June 5, 2025

DOI: 10.3892/wasj.2025.365

Abstract. Breast cancer is one of the most prevalent diseases affecting the female population, with its incidence increasing globally. Previous studies have identified cyclins, CDKs and upstream signaling molecules as key therapeutic targets, as their overexpression can drive the transformation of normal cells into cancerous ones. Sulfated galactan (SG), a polysaccharide derived from *Gracilaria fisheri*, has demonstrated potential in modulating cellular functions. Recent research suggests that low molecular weight SG (LSG), when supplemented with an octanoyl ester (LSGO), exhibits an enhanced biological activity. However, the anticancer effects of SG and its derivatives in breast cancer remain underexplored. The present study thus aimed to examine the effects of SG, LSG and LSGO on MCF-7 breast cancer cells. Cytotoxicity was initially assessed in L929 normal fibroblast cells and MCF-7 cells. While all three forms were non-toxic to L929 cells, LSGO exhibited slight cytotoxicity and significantly induced cell cycle arrest at the G2/M phase. Mechanistically, LSGO suppressed the PI3K/AKT/mTOR and ERK pathways, downregulated cyclins and CDKs, and led to cell cycle arrest and reduced cell proliferation. These results suggest that the structural modification of SG enhances its anti-proliferative capacity, highlighting LSGO as a promising candidate for the treatment of MCF-7 cells. Overall, these findings provide insight into the molecular mechanisms by which SG derivatives affect breast cancer cell proliferation and underscore their potential as anti-proliferative agents targeting cell cycle regulatory proteins.

Correspondence to: Dr Tawut Rudtanatip, Electron Microscopy Unit, Department of Anatomy, Faculty of Medicine, Khon Kaen University, 123 Moo 16 Thanon Mittraphap, Mueang, Khon Kaen 40002, Thailand
E-mail: tawut@kku.ac.th

Key words: Gracilaria fisheri, sulfated galactan derivatives, MCF-7 cell, anti-proliferation, cell cycle arrest

Introduction

The majority of types of cancer, including breast cancer, result from genetic and epigenetic alterations that disrupt normal cellular signaling, leading to uncontrolled proliferation and survival (1-3). Key pathways involved in breast cancer progression include the phosphoinositide 3-kinase (PI3K)/protein kinase B (AKT)/mammalian target of rapamycin (mTOR) and mitogen-activated protein kinase (MAPK)/extracellular signal-regulated kinase (ERK) signaling cascades, which not only drive tumorigenesis, but also contribute to chemotherapeutic resistance (4,5). These pathways regulate cell cycle progression by stimulating cyclin D1, a critical protein that promotes cell division (6). The cell cycle, which consists of four phases (G0/G1, S, G2 and M) (7), is regulated by cyclins and cyclin-dependent kinases (CDKs) that form cyclin/CDK complexes (8). This process is negatively regulated by CDK inhibitors, such as p21, which suppress cyclin/CDK activity (9). The dysregulation of p21 or the overexpression of cyclins and CDKs can lead to uncontrolled cell proliferation, a hallmark of cancer (8). Notably, cyclin D1 and CDK4/6 are overexpressed in breast cancer, along with elevated levels of the proliferation marker, Ki-67 (10). Ki-67 levels rapidly decrease during cancer cell apoptosis following treatment with chemotherapy (11). However, the adverse effects of chemotherapy on normal cells often limit its therapeutic success (12).

Natural products are increasingly being explored for their anticancer potential due to their fewer adverse effects. Sulfated galactan (SG), a polysaccharide isolated from the red seaweed, *Gracilaria fisheri* (*G. fisheri*), has been shown to induce cell cycle arrest in cholangiocarcinoma (CCA) by downregulating cyclin and CDK expression, while upregulating tumor suppressors, such as p21 and p53 (13). It has also been reported to suppress CCA cell invasion and migration (14). Additionally, chemical modifications, such as reducing molecular weight and substituting functional groups, have been found to enhance the anticancer properties of polysaccharides (15). In a recent study, modified SG from *G. fisheri* with low molecular weight (LSG), supplemented with an octanoyl ester (LSGO), was found to exhibit an enhanced wound healing activity (16).

However, the effects of SG and its derivatives, including LSG and LSGO, on breast cancer remain unexplored. Therefore, the present study aimed to evaluate the anticancer activities of SG and its derivatives in the MCF-7 breast cancer cell line. The mechanisms by which SG and its derivatives affect MCF-7 cell proliferation, cell cycle regulation, protein expression and mRNA expression were also investigated.

Materials and methods

Cell lines and cell culture. Human mammary gland epithelial adenocarcinoma (MCF-7; cat. no. HTB-22) and normal fibroblast (L929; cat. no. CCL-1) cell lines were purchased from the American Type Culture Collection (ATCC). MCF-7 cells were cultured in Dulbecco's modified Eagle's medium (DMEM; Gibco™, Thermo Fisher Scientific, Inc.) containing L-glutamine, pyridoxine hydrochloride and sodium bicarbonate ($NaHCO_3$), supplemented with 10% fetal bovine serum (FBS; Invitrogen, Thermo Fisher Scientific, Inc.) and 1% antibiotic-antimycotic (penicillin/streptomycin; Invitrogen, Thermo Fisher Scientific, Inc.). L929 cells were cultured in minimum essential medium (MEM; Gibco™, Thermo Fisher Scientific, Inc.), which contains L-glutamine and phenol red, supplemented with 10% FBS and 1% antibiotic-antimycotic. Both MCF-7 and L929 cells were maintained under standard conditions at 37˚C in a humidified atmosphere of 5% CO_2.

Evaluation of the cytotoxicity of SG and its derivatives in MCF-7 and L929 cells. SG, LSG and LSGO were prepared as previously described by Rudtanatip *et al* (16). MTT assay was used to assess the cytotoxicity of SG, LSG and LSGO in MCF-7 and L929 cell cultures. MCF-7 and L929 cells were seeded into 96-well plates at a density of $2x10^4$ cells/well and allowed to attach for 24 h under standard incubator conditions. The cells were then treated with various concentrations of SG, LSG and LSGO (0, 125, 250, 500 and 1,000 μg/ml), as well as paclitaxel (PTX; Intaxel® 6 mg/ml paclitaxel injection, Fresenius Kabi) and gemcitabine (GEM; gemcitabine hydrochloride, Supelco, MilliporeSigma) (0, 0.2, 0.4, 0.6, 0.8 and 1 μg/ml) for 48 h. PTX and GEM served as the positive controls, while untreated cells were used as the normal control. Following the treatment period, 20 μl MTT solution (5 mg/ml; MilliporeSigma) were added to each well and incubated for 3 h at 37˚C. The medium was then removed, and 100 μl dimethyl sulfoxide (DMSO; RCI Labscan™ Limited) were added to dissolve the purple formazan crystals. The plate was shaken on a microplate shaker for 20 min, and the absorbance was measured at 540 nm using a microplate reader (Varioskan® LUX, cat. no. N16044; Thermo Fisher Scientific, Inc.). The results were reported as IC_{50} values, as previously described (13). The concentrations of SG and its derivatives, as well as those of PTX and GEM used in the present study were based on a previous study by the authors and other relevant studies (16-18).

Evaluation of cell morphology. The morphology of the MCF-7 and L929 cells treated with PTX, GEM, SG, LSG and LSGO was also examined. The MCF-7 and L929 cells ($6x10^4$ cells/well) were cultured in a 24-well plate for 24 h, and the cells were divided into six groups as follows: i) The normal control (NC), no treatment; ii) PTX, cells were treated with 0.5 μg/ml PTX; iii) GEM, cells were treated with 0.5 μg/ml GEM; iv) SG, cells were treated with 500 μg/ml SG; v) LSG, cells were treated with 500 μg/ml LSG; and vi) LSGO, cells were treated with 500 μg/ml LSGO. The cells were treated with 2 ml of the respective solution and incubated for 48 h at 37˚C before observing cell morphology under a Nikon ECLIPSE TS100 inverted microscope (Nikon Corporation). Cell counts were analyzed in three randomly selected fields at x200 magnification using ImageJ software version 1.54g (National Institutes of Health).

A concentration of 500 μg/ml was selected for use in subsequent assays, as both 500 and 1,000 μg/ml exerted comparable moderate effects on cell viability without reaching the IC_{50} value. The results of MTT assay confirmed that 500 μg/ml produced similar outcomes to 1,000 μg/ml, supporting its use in further experiments.

Evaluation of the anti-proliferative effect of SG and its derivatives on MCF-7 cells. The results of cytotoxicity assay indicated that although SG and its derivatives were not markedly cytotoxic to the MCF-7 cells, they reduced cell numbers by 20% compared to the control. This suggests that SG and its derivatives may inhibit MCF-7 cell proliferation, as previously reported (13). The anti-proliferative effects of SG and its derivatives were further investigated.

Experimental design. The MCF-7 cells were cultured and divided into six groups as follows: i) NC, no treatment; ii) PTX, cells were treated with 0.5 μg/ml paclitaxel; iii) GEM, cells were treated with 0.5 μg/ml GEM; iv) SG, cells were treated with 500 μg/ml SG; v) LSG, cells were treated with 500 μg/ml LSG; and vi) LSGO, cells were treated with 500 μg/ml LSGO.

Hoechst/propidium iodide (PI) dual staining. The cytotoxic effects of SG and its derivatives were further confirmed using Hoechst/PI dual staining. The MCF-7 cells were plated on round coverslips in a 24-well plate at a density of $6x10^4$ cells/well in DMEM and incubated for 24 h at 37˚C. Following incubation, the cells were treated with the respective solution for 48 h. The cells were then washed with PBS and stained with Hoechst (Merck KGaA) and PI (BioChemica, PanReac AppliChem) at a 1:1 ratio for 30 min at room temperature. After staining, the cells were washed three times with PBS in the dark. The coverslips containing the stained cells were then mounted on glass slides with a droplet of anti-fade solution. Finally, the cells were observed under a confocal microscope (ZEISS LSM 800, Carl Zeiss AG), as previously described (16). The laser intensity wavelengths were 405 nm with a pinhole size of 1.18 AU/45 μm for Hoechst staining and 561 nm with a pinhole size of 0.90 AU/47 μm for PI staining. PI fluorescent intensity was measured in three randomly selected fields at a x200 total magnification using ImageJ software version 1.54g (National Institutes of Health).

Immunofluorescence staining of cell proliferation using the Ki-67 biomarker. The MCF-7 cells seeded on round coverslips in a 24-well plate were treated with the respective solution for 48 h. Following treatment, the cells were fixed with 4% paraformaldehyde in 0.1% Triton X-100 at room temperature

for 15 min and were then washed three times with PBS. Subsequently, the cells were blocked with 5% bovine serum albumin (BSA; Capricorn Scientific GmbH) for 30 min at room temperature. After blocking, the cells were washed with PBS and incubated overnight at 4˚C with a primary antibody specific to mouse anti-Ki-67 (dilution 1:500; cat no. 14569982; Invitrogen, Thermo Fisher Scientific, Inc.). The following day, the cells were incubated with a fluorescent-labeled secondary antibody (goat anti-mouse FITC-conjugated; dilution 1:500; cat no. AP308F; Merck Millipore) for 1 h, at room temperature in the dark. Following incubation, the cells were washed with PBS in the dark and counterstained with Cell Mask™ Deep Red plasma membrane stain (dilution 1:500; cat no. C10066; Invitrogen, Thermo Fisher Scientific, Inc.) for 20 min at room temperature. A total of 5 μl of antifade solution conjugated with DAPI dye (ProLong™ Diamond Antifade Mountant with DAPI, Invitrogen, Thermo Fisher Scientific, Inc.) was then added to a glass slide. The round coverslips containing the cells were then placed on the glass slide with a droplet of antifade solution. Finally, the fluorescence intensity of Ki-67 was observed using a confocal microscope (ZEISS LSM 800, Carl Zeiss AG), as previously described (19).

Evaluation of cell cycle arrest using flow cytometry. A flow cytometry cell cycle arrest assay was used to evaluate the mechanisms of action of SG and its derivatives. The MCF-7 cells were seeded in a six-well plate at a density of $1.5x10^5$ cells/well and allowed to adhere overnight. The cells were then treated with PTX, GEM, SG, LSG and LSGO solutions for 48 h. Following treatment, all adherent cells were harvested by trypsinization, transferred to sterile Eppendorf tubes, and centrifuged at 2,795 x g at 4˚C for 5 min to pellet the cells. The cell pellets were washed three times with cold PBS and centrifuged at 2,795 x g at 4˚C for 5 min. The supernatant was discarded, and ice-cold 70% ethanol was added to fix the cells. The pellets were then resuspended to obtain a single-cell suspension and incubated at -20˚C for 1 week. Following incubation, the cell pellets were washed three times with PBS, and the supernatant was removed. Nuclei were stained with PI/RNase staining solution (FxCycle™ PI/RNase, Thermo Fisher Scientific, Inc.) and incubated for 40 min in the dark at room temperature. Flow cytometric analysis was performed using a FACSCanto II flow cytometer (Model FACSCanto II, BD Biosciences). The percentage of cells in each phase of the cell cycle was then analyzed (20).

Analysis of mRNA expression using reverse transcription-quantitative PCR (RT-qPCR). TRIzol reagent (200 μl; MilliporeSigma) was used for RNA extraction. RNA purity and concentration were determined by measuring the absorbance ratio at 260/280 nm using a NanoDrop 2000 spectrophotometer (Thermo Fisher Scientific, Inc.). Complementary DNA (cDNA) was synthesized from 1 μg RNA using the RevertAid First Strand cDNA Synthesis kit (Thermo Fisher Scientific, Inc.) through incubation at 42˚C for 60 min, followed by heating at 70˚C for 5 min. Subsequently, mRNA expression was analyzed using qPCR with the synthesized cDNA and PCR Master Mix (Molecular Biology, Thermo Fisher Scientific, Inc.), and forward and reverse primers. The cycling conditions were as follows: 50˚C for 2 min, 95˚C for 10 min, followed by 40 cycles of 95˚C for 15 sec, 60˚C for 30 sec and 72˚C for 30 sec. Data quantification calculated using the $2^{-\Delta\Delta Cq}$ method (21) was performed using the Bio-Rad CFX Maestro software (Bio-Rad Laboratories, Inc.). The primers used in the present study included Ki-67, PI3K, AKT, mTOR, cyclin D1, CDK4, cyclin A, CDK2, p21, ERK 1/2 and GAPDH (Bionics). Forward and reverse primer sequences were designed using NCBI/Primer-Blast, and their sequences are provided in Table I.

Analysis of protein expression. The expression of proteins involved in cell proliferation was determined after the MCF-7 cells were treated for 48 h using western blot analysis. Cells were harvested for protein extraction. The protein concentration was quantified using a NanoDrop 2000 spectrophotometer (Thermo Fisher Scientific, Inc.), and 50 μg protein samples were separated by electrophoresis using 12% sodium dodecyl sulfate polyacrylamide gel electrophoresis (SDS-PAGE). The separated proteins were then transferred onto a nitrocellulose membrane (Amersham™ Protran™ Premium 0.45 μm NC nitrocellulose western blotting membranes), which was blocked with 4% BSA for 1 h at room temperature. Each membrane was probed with primary antibodies (dilution 1:1,000) against mouse anti-Ki-67 (cat. no. 14569982; Invitrogen, Thermo Fisher Scientific, Inc.), rabbit anti-PI3K (cat. no. 4255S; Cell Signaling Technology, Inc.), rabbit anti-phosphorylated (p)-AKT (cat. no. sc-135651; Santa Cruz Biotechnology, Inc.), rabbit anti-AKT (cat. no. 8596S; Cell Signaling Technology, Inc.), rabbit anti-p-mTOR (cat. no. 5536S; Cell Signaling Technology Inc.), rabbit anti-mTOR (cat. no. 2972S; Cell Signaling Technology Inc.), mouse anti-cyclin D1 (cat. no. AHF0082; Invitrogen, Thermo Fisher Scientific, Inc.), mouse anti-CDK4 (cat. no. AHZ0202; Invitrogen, Thermo Fisher Scientific, Inc.), rabbit anti-p21 (cat. no. E2R7A; Cell Signaling Technology Inc.), rabbit anti-cyclin A (cat. no. AF0142; Affinity Biosciences), rabbit anti-CDK2 (cat. no. MA5-17052; Invitrogen, Thermo Fisher Scientific, Inc.), mouse anti-ERK1/2 (cat. no. 9102S; Cell Signaling Technology Inc.) and rabbit anti-β-actin (cat. no. AF7018; Affinity Biosciences) and incubated overnight at 4˚C. The membranes were then incubated with a secondary antibody conjugated with horseradish peroxidase (dilution 1:2,000; cat. no. 31460 for anti-rabbit antibody and cat. no. 626520 for anti-mouse antibody; Invitrogen, Thermo Fisher Scientific, Inc.) at room temperature for 1 h. Following incubation, the membranes were washed with Tris-buffered saline-Tween 20 (TBS-T) solution, and immunoreactivity was enhanced using a chemiluminescence ECL-Western blotting substrate kit (Clarity™ Western ECL substrate, Bio-Rad, USA). Finally, protein bands were detected using the ChemiDoc Touch imaging system (Amersham™ ImageQuant™ 800 biomolecular imager, Cytiva). Relative protein expression was quantified using ImageJ software version 1.32j (National Institutes of Health) with band intensities standardized to β-actin (22).

Statistical analysis. All experiments were performed in triplicate, and data are presented as the mean ± SEM. Statistical analysis was conducted using one-way ANOVA followed by Tukey's multiple comparisons test using GraphPad Prism software version 5 (Dotmatics).

Table I. Nucleotide sequences of specific primers used for mRNA expression.

Gene names	Primers	Nucleotide sequences (5' to 3')
Ki-67	Forward	GAAAGAGTGGCAACCTGCCTTC
	Reverse	GCACCAAGTTTTACTACATCTGCC
PI3K	Forward	AACACAGAAGACCAATACTC
	Reverse	TTCGCCATCTACCACTAC
AKT	Forward	TCTATGGCGCTGAGATTGTG
	Reverse	CTTAATGTGCCCGTCCTTGT
mTOR	Forward	GCTTGATTTGGTTCCCAGGAC
	Reverse	GTGCTGAGTTTGCTGTACCCA
Cyclin D1	Forward	GCATGTTCGTGGCCTCTAAG
	Reverse	CGTGTTTGCGGATGATCTGT
CDK4	Forward	TGAGGGTCTCCCTTGATCTGAG
	Reverse	AGGGATACATCTCGAGGCCA
p21	Reverse	GCTTCATGCCAGCTACTTCC
	Forward	CCCTTCAAAGTGCCATCTGT
Cyclin A	Forward	GTCAGAGAGGGGATGGCAT
	Reverse	CCAGTCCACCAGAATCGTG
CDK2	Forward	GAATCTCCAGGGAATAGGGC
	Reverse	CTGAAATCCTCCTGGGCTG
ERK1/2	Forward	TGGCAAGCACTACCTGGATCAG
	Reverse	GCAGAGACTGTAGGTAGTTTCGG
GAPDH	Reverse	GGTGAAGGTCGGTGTGAACG
	Forward	CTCGCTCCTGGAAGATGGTG

Results

Effects of SG and its derivatives on the viability of MCF-7 and L929 cells. The cytotoxic effects of SG and its derivatives on MCF-7 breast cancer and L929 normal fibroblast cells were evaluated and expressed as a percentage of the control following 48 h of exposure at concentrations of 125, 250, 500 and 1,000 μg/ml. The results revealed that at 500 and 1,000 μg/ml, MCF-7 cell viability significantly decreased from 100 to 80% (Fig. 1A), while L929 cell viability exhibited no significant differences between the groups (Fig. 1B). However, the IC_{50} values of SG, LSG and LSGO in the MCF-7 cells were calculated to be 3,027, 2,416 and 1,757 μg/ml, respectively. Additionally, the anticancer drugs, PTX and GEM, were used as positive controls to compare the cytotoxic effects. PTX and GEM significantly reduced the viabilities of both the MCF-7 and L929 cells, with low IC_{50} values of 0.54 and 0.57 μg/ml, respectively (Fig. 1C and D). Cell morphology observed under a phase contrast microscope revealed that the MCF-7 and L929 cells treated with PTX and GEM (Fig. 1E and F) exhibited characteristic cellular changes, including shrinkage, membrane bleb formation and the loss of normal shape. Notably, the L929 cells treated with SG and its derivatives did not exhibit any noticeable changes compared to the control. Moreover, the quantitative cell counts of MCF-7 and L929 cells following treatment, shown in Fig. 1G and H, were consistent with the results of MTT assay. These findings suggest a selective effect of the compounds on cancer cells without affecting normal cells.

Determination of the death and proliferation of MCF-7 cells caused by SG and its derivatives. The decreased viability of the MCF-7 breast cancer cells following treatment with SG and its derivatives may be associated with cell death and/or inhibited cell proliferation. To investigate this, immunofluorescence staining was performed using Hoechst/PI dual staining and the Ki-67 biomarker. The results revealed that the cells treated with 500 μg/ml SG and its derivatives exhibited a slight increase in fluorescent PI intensity compared to the normal control, consistent with the effects observed in the PTX- and GEM-treated cells (Fig. 2). By contrast, treatment with 500 μg/ml SG and its derivatives resulted in a significant reduction in the fluorescent Ki-67 intensity compared to the normal control, aligning with the results observed in the PTX- and GEM-treated cells (Fig. 3A). Additionally, the mRNA and protein expression levels of Ki-67 were significantly decreased in the MCF-7 cells treated with SG derivatives, particularly LSGO (Fig. 3B and C), corresponding to the effects observed with PTX and GEM. These findings suggest that SG and its derivatives exert anti-proliferative effects on MCF-7 cells.

SG derivatives promote MCF-7 cell cycle arrest. The present study further investigated the anti-proliferative effects of SG and its derivatives on MCF-7 cells by analyzing the DNA content across different cell cycle phases using PI staining. Flow cytometry profiles of the nuclear DNA content revealed alterations in cell population distribution across phases following treatment with SG and its derivatives compared to the normal control (untreated cells), as shown in Fig. 4. In the

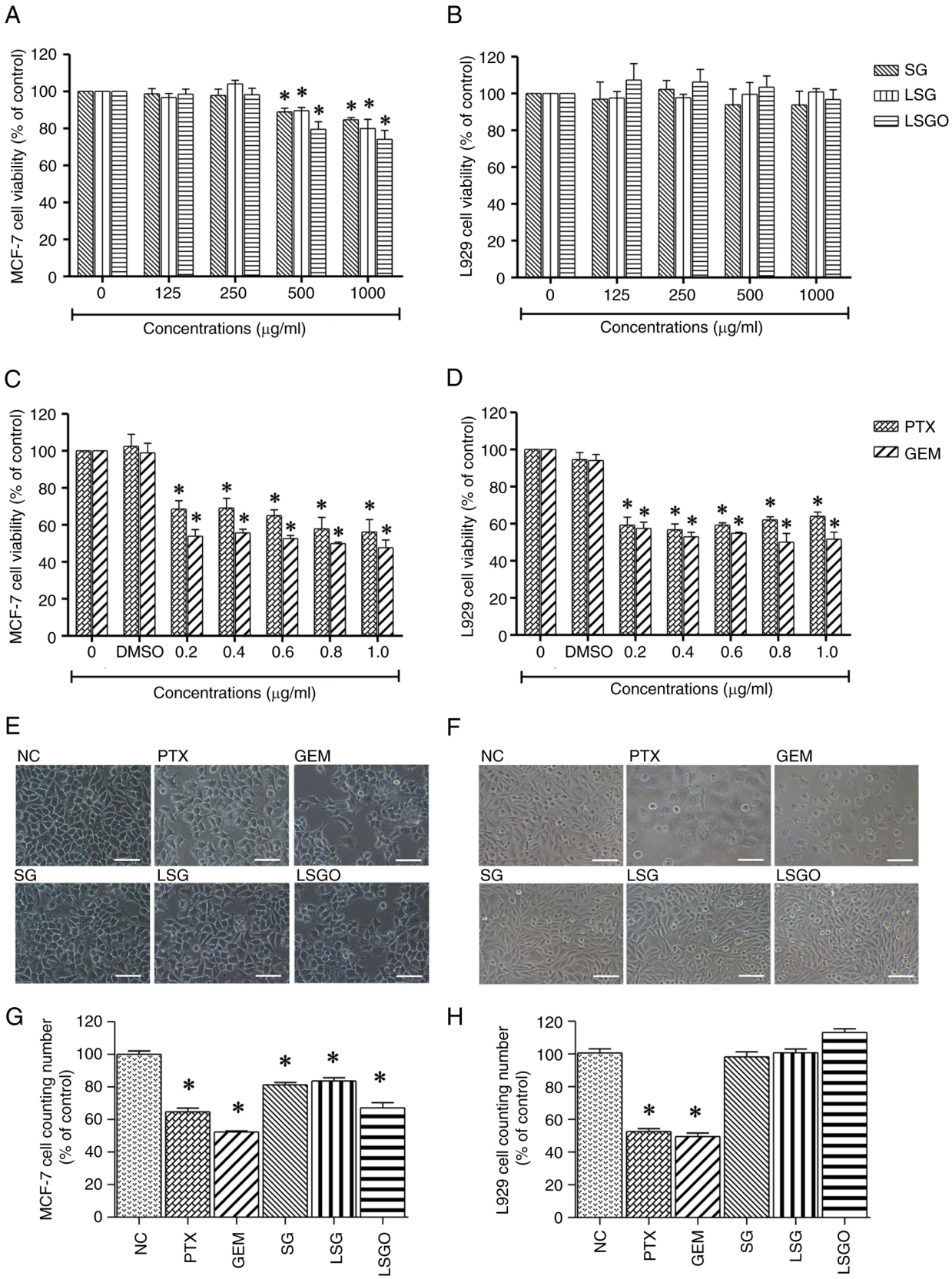

Figure 1. Effects of PTX and GEM (at concentrations of 0.2, 0.4, 0.6, 0.8 and 1.0 μg/ml) and SG, LSG and LSGO (at concentrations of 125, 250 500, and 1,000 μg/ml) on the viability of MCF-7 breast cancer cells and L929 normal fibroblast cells, as assessed using MTT assay. (A) Viability of MCF-7 cells treated with SG, LSG and LSGO. (B) Viability of L929 cells treated with SG, LSG and LSGO. (C) Viability of MCF-7 cells treated with PTX and GEM. (D) Viability of L929 cells treated with PTX and GEM. (E) Phase-contrast images illustrating morphological changes in MCF-7 cells following treatment with PTX, GEM, SG, LSG and LSGO. (F) Phase-contrast images illustrating morphological changes in L929 cells following treatment with PTX, GEM, SG, LSG and LSGO. Scale bars, 100 μm. (G) Quantitative cell counts of MCF-7 cells treated with PTX, GEM, SG, LSG and LSGO. (H) Quantitative cell counts of L929 cells treated with PTX, GEM, SG, LSG and LSGO. The results are presented as the mean±SEM (n=3) from three independent experiments. *P<0.05, statistically significant difference compared to the normal control at a 95% confidence level. PTX, paclitaxel; GEM, gemcitabine; SG, sulfated galactan; LSG low molecular weight SG; and LSGO, octanoyl ester-supplemented SG.

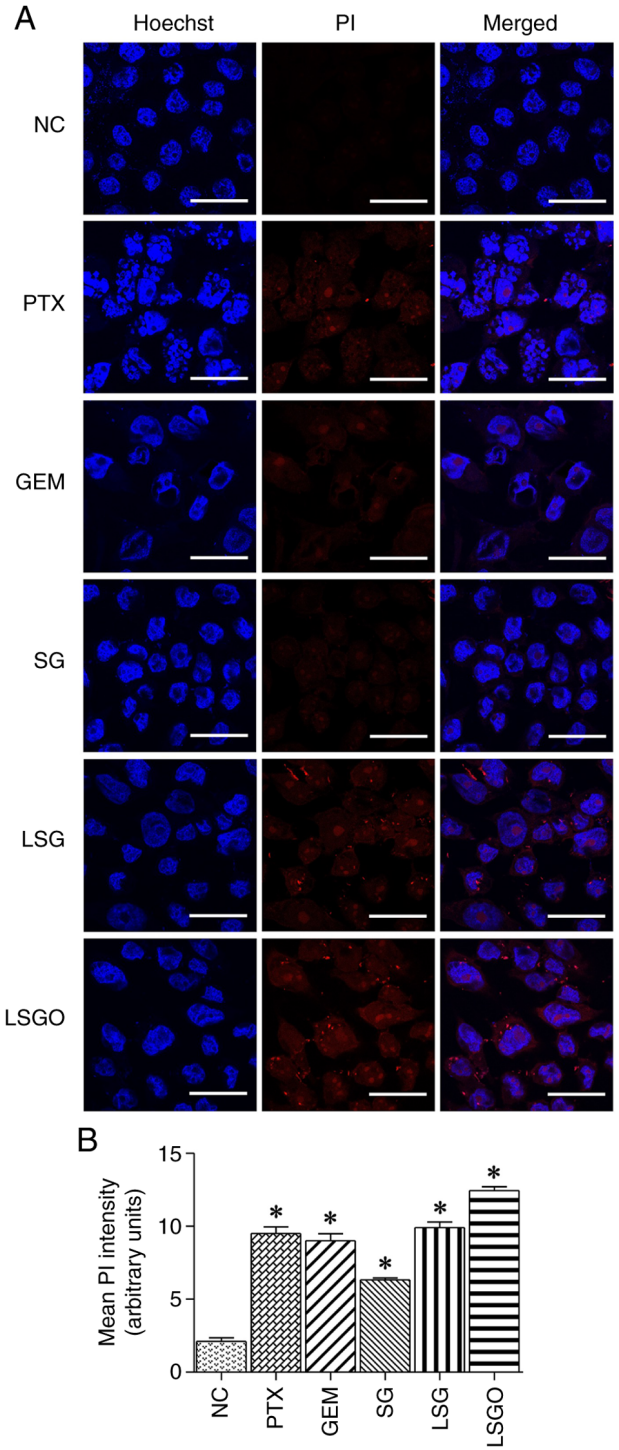

Figure 2. Hoechst/PI dual staining in MCF-7 cells following treatment with PTX, GEM, SG, LSG and LSGO. (A) Immunofluorescence confocal micrographs illustrating the intensity levels of Hoechst and PI dual staining in MCF-7 cells following treatment. Scale bars, 20 μm. (B) Mean fluorescence PI intensity in MCF-7 cells following treatment. The results are presented as the mean ± SEM (n=3) from three independent experiments. *P<0.05, statistically significant difference compared to the normal control at a 95% confidence level. PTX, paclitaxel; GEM, gemcitabine; SG, sulfated galactan; LSG low molecular weight SG; and LSGO, octanoyl ester-supplemented SG.

normal control, the cells in the sub-G1/G1 phase accounted for 61.70%, the S phase for 20.87% and the G2/M phase for 17.50%. However, the cells treated with SG and its derivatives exhibited a decrease in the number of cells in the sub-G1/G1 phase, a slight increase in the number of cells in the S phase, and a significant increase in the number of cells in the G2/M phase compared to the normal control. Specifically, in the SG group, the number of cells in the sub-G1/G1, S and G2/M phases were 57.70, 22.73 and 19.53%, respectively. In the LSG group, the number of cells in the sub-G1/G1, S and G2/M phases were 55.74, 22.6 and 21.70%, respectively, while in the LSGO group, the number of cells in the sub-G1/G1, S and G2/M phases were 56.73, 22.03 and 21.20%, respectively. This increase in G2/M phase arrest was consistent with the results observed in the PTX-treated group. Additionally, the analysis of GEM-treated cells revealed a higher percentage of cells in the sub-G1/G1 phase compared to the other phases. These findings suggest that SG derivatives may effectively inhibit MCF-7 cell proliferation by inducing cell cycle arrest at the G2/M phase.

Decreased expression of mRNA and proteins involved in MCF-7 cell cycle arrest caused by SG derivatives. The expression of key mRNA and proteins involved in tumor cell proliferation in MCF-7 cells, including those in the PI3K/Akt/mTOR, MAPK and CDK pathways, was assessed following treatment with SG and its derivatives using RT-qPCR and western blot analysis. Compared to the controls, the expression levels of PI3K/Akt/mTOR, MAPK and CDKs were altered in the cells treated with SG and its derivatives, in accordance with the effects observed in the PTX- and GEM-treated groups. The results of RT-qPCR revealed that the mRNA expression levels of PI3K, AKT, mTOR, cyclin D1, CDK4, cyclin A, CDK2 and ERK were significantly decreased in the cells treated with LSGO compared to the normal control (Fig. 5). Similarly, as demonstrated in Fig. 6, the protein expression levels of PI3K, p-AKT/AKT, p-mTOR/mTOR, cyclin D1, CDK4, cyclin A, CDK2 and ERK were significantly decreased in the cells treated with LSGO compared to the NC. However, the expression levels of some proteins (p-mTOR/mTOR, CDK2 and ERK) were unaltered in the cell treated with SG and LSG. Of note, p21 expression remained unaltered at both the mRNA and protein levels in the cells treated with SG derivatives. Notably, treatment with LSGO exerted a significantly greater reduction in both mRNA and protein expression levels, suggesting a superior anti-proliferative effect of LSGO on MCF-7 cells.

Discussion

Breast cancer remains one of the most prevalent malignancies worldwide (23). Despite advancements being made in treatment strategies, managing the disease remains challenging, with chemotherapeutic resistance and associated side-effects often leading to treatment failure (24). In response, researchers are exploring the potential of natural compounds in breast cancer therapy, particularly for mitigating chemotherapy-induced side-effects. Previous studies have demonstrated that polysaccharides inhibit cancer cell proliferation and survival by inducing cell cycle arrest and apoptosis. For instance, serum collected from fucoidan-treated rats was shown to inhibit the proliferation and increase the apoptosis of MCF-7 cells (25). Fucoidan from the brown algae, *Fucus vesiculosus,* at concentrations ranging from 100 to 300 μg/ml, has also been

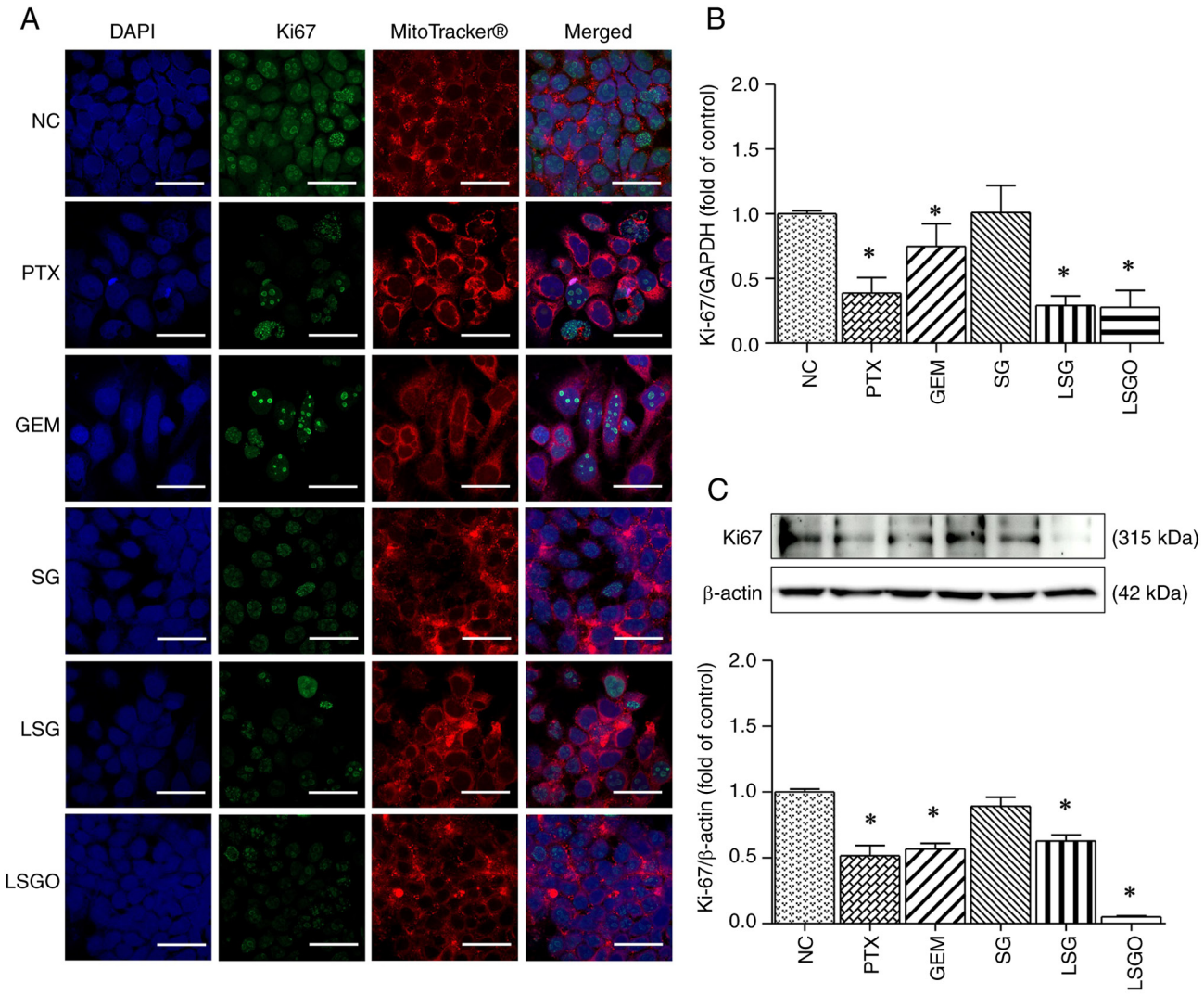

Figure 3. Expression levels of Ki-67 in MCF-7 cells following treatment with PTX, GEM, SG, LSG and LSGO. (A) Immunofluorescence confocal micrographs illustrating Ki-67 expression in MCF-7 cells. Ki-67 protein is shown in green, nuclei were stained with DAPI (blue), and the cell plasma membrane was stained with MitoTracker® Deep Red (red). Scale bars, 20 μm. (B) mRNA expression levels of Ki-67 in MCF-7 cells, assessed using reverse transcription-quantitative PCR. (C) Protein expression levels of Ki-67 in MCF-7 cells, assessed using western blot analysis. The results are presented as the mean ± SEM (n=3) from three independent experiments. *P<0.05, statistically significant difference compared to the normal control at a 95% confidence level. PTX, paclitaxel; GEM, gemcitabine; SG, sulfated galactan; LSG low molecular weight SG; and LSGO, octanoyl ester-supplemented SG.

reported to induce apoptosis and promote cell cycle arrest in CL-6 CCA cells by increasing the levels of apoptotic protein markers and decreasing the expression of cyclin and CDK molecules (26). SG, extracted from the red algae, *G. fisheri*, is a sulfated polysaccharide (SP) with a galactose backbone and a high percentage of sulfate groups (27). It has been shown to inhibit cell proliferation and induce cell cycle arrest in HuCCA-1 cells by downregulating cyclin/CDK expression following treatment at concentrations of 10 and 50 μg/ml (13). Thus, the anticancer activity of polysaccharides may be influenced by several factors, including their molecular structure, dosage and the type of cancer cells involved (28). Additionally, reducing molecular weight (15,29) and supplementing SP with an octanoyl ester (16) have been found to enhance their biological effectiveness. In the present study, the anticancer activity of SG from *G. fisheri*, along with its structurally modified derivatives, LSG and LSGO, was investigated in MCF-7 breast cancer cells and L929 normal lung fibroblasts. The effects were compared with those of unmodified SG and the anticancer drugs, PTX and GEM. The concentrations used for SG and its derivatives (125-1,000 μg/ml) in the present study reflect typical dosing ranges for marine polysaccharides (17), which generally exhibit lower cytotoxicity per unit mass compared to small-molecule drugs such as PTX and GEM (0.2-1 μg/ml) (18). This difference in dosage is necessary due to variations in molecular size, bioavailability and mechanisms of action.

The results of the present study demonstrated that SG and its derivatives decreased cell viability and suppressed MCF-7 cell proliferation, in accordance with the reduced Ki-67 expression and the induction of cell cycle arrest, particularly in the cells treated with LSGO, similar to the effects observed with PTX and GEM. Treatment with LSGO in MCF-7 cells exerted a greater anti-proliferative effect, indicating that its molecular structure is positively associated with its biological activity (30). Furthermore, the

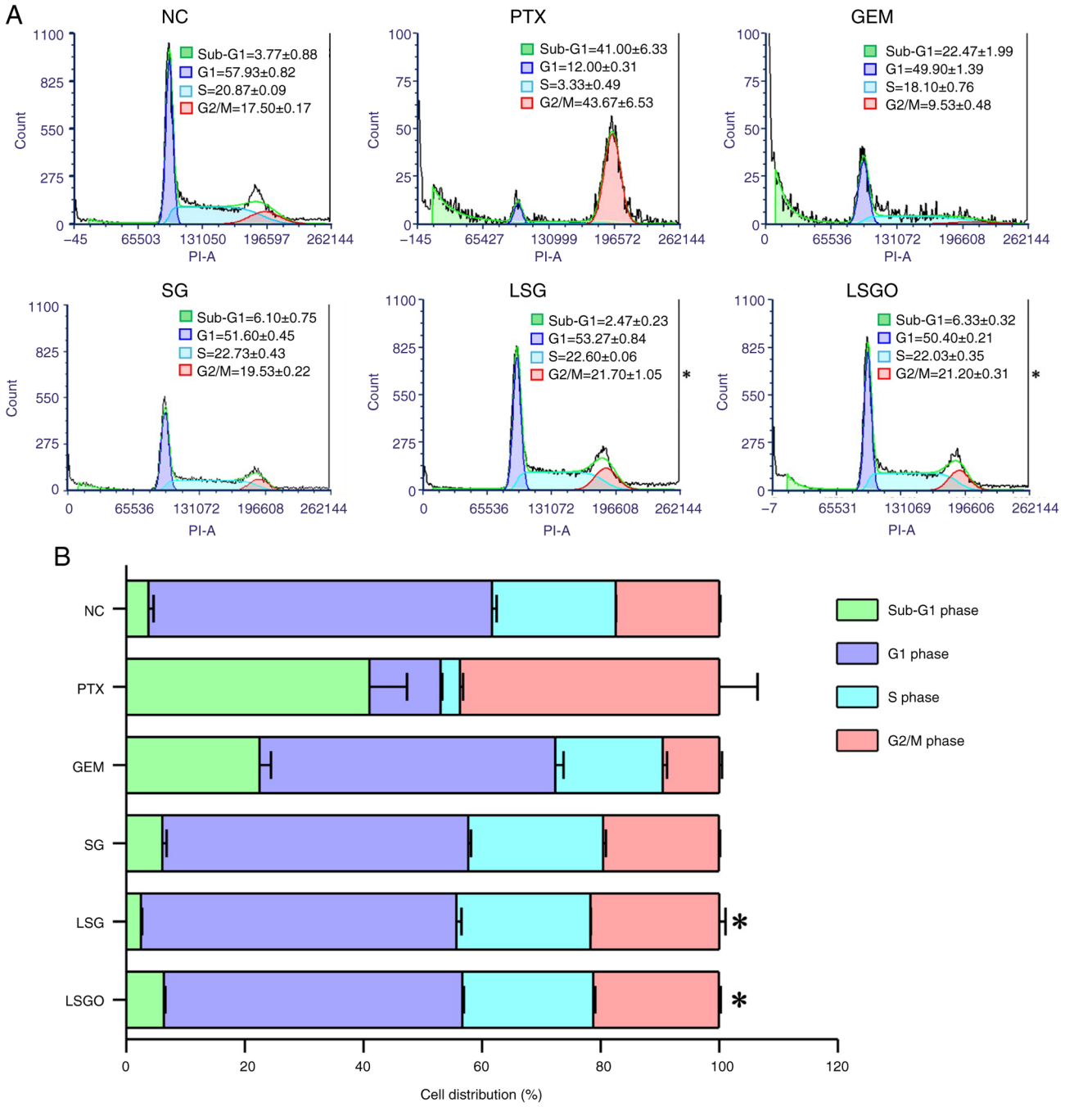

Figure 4. Effects of PTX, GEM, SG, LSG and LSGO on the cell cycle distribution of MCF-7 cells, assessed using flow cytometry. (A) Representative histograms depicting cell cycle distribution in MCF-7 cells following treatment. (B) Quantitative results demonstrating the percentage of cells in each cell cycle phase for the normal control and treatment groups. The results are presented as the mean±SEM (n=3) from three independent experiments. *P<0.05, statistically significant difference compared to the normal control at a 95% confidence level. PTX, paclitaxel; GEM, gemcitabine; SG, sulfated galactan; LSG low molecular weight SG; and LSGO, octanoyl ester-supplemented SG.

enhanced anti-proliferative activity of LSGO suggests that it may improve cellular internalization, thereby increasing its overall efficacy (31). A high Ki-67 expression has been shown to be associated with cancer proliferation and it is a well-established indicator of prognosis and clinical outcomes (32). Since Ki-67 remains active during the G1, S, G2 and M phases of the cell cycle, it serves as a reliable marker of cell proliferation and a recognized hallmark of oncogenesis (33). Notably, the decreased Ki-67 expression through antisense oligonucleotides has been shown to inhibit cancer cell proliferation and tumor growth (34). Herein, the reduction of Ki-67 expression in MCF-7 cells following SG and its derivatives treatment suggests anti-proliferative activity, consistent with previous findings on polysaccharides extracted from *Crataegus* (Hawthorn), which inhibited human colon cancer HCT116 cell proliferation by reducing Ki-67 protein expression and inducing cell cycle arrest (35). However, these effects were not observed in L929 normal fibroblasts, indicating a selective effect on breast cancer cells (36). This selectivity may be attributed to differences

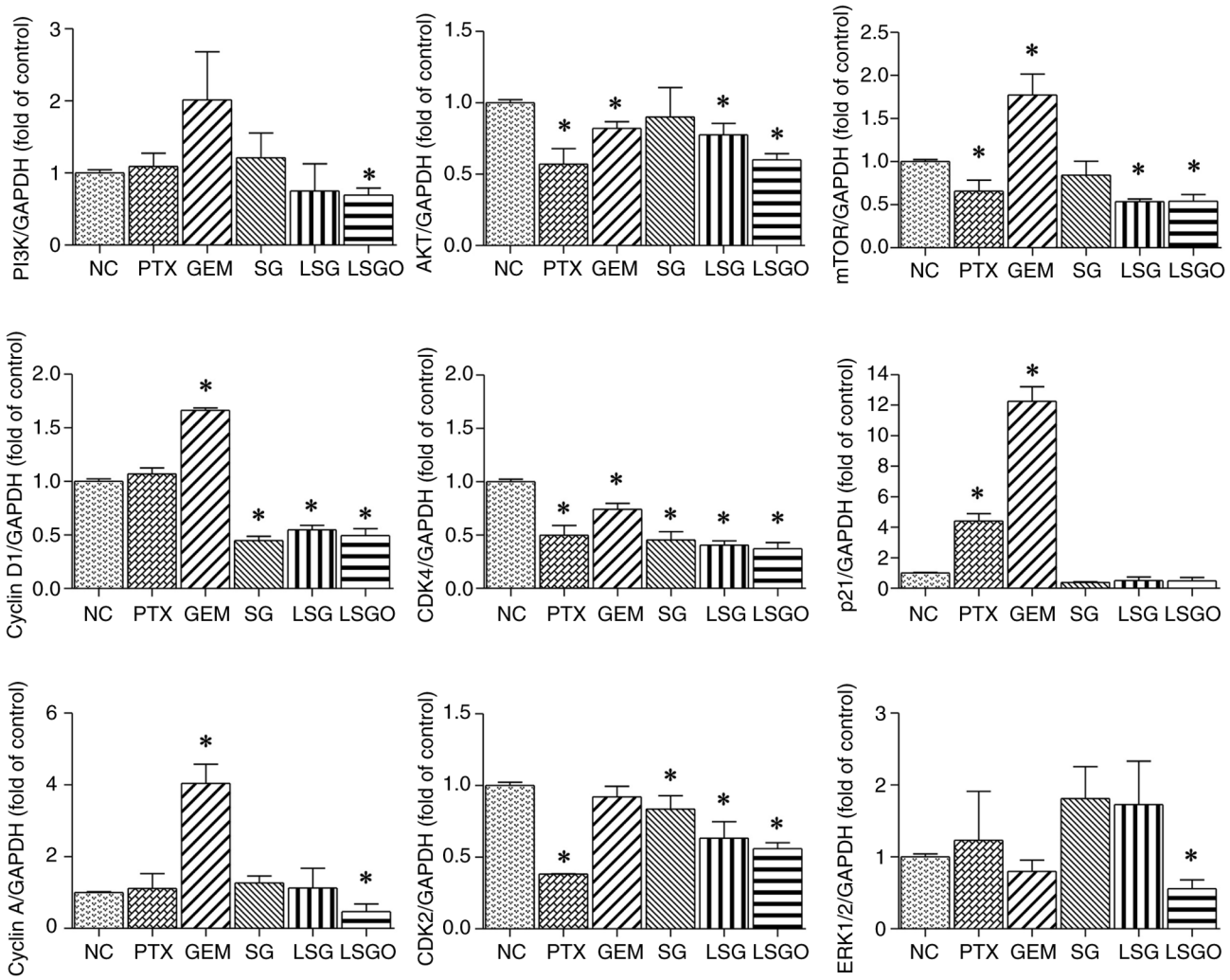

Figure 5. mRNA expression levels of PI3K, AKT, mTOR, cyclin D1, CDK4, p21, cyclin A, CDK2 and ERK 1/2 in MCF-7 cells treated with PTX, GEM, SG, LSG and LSGO, assessed relative to GAPDH using reverse transcription-quantitative PCR. The results are presented as the mean±SEM (n=3) from three independent experiments. *P<0.05, statistically significant difference compared to the normal control at a 95% confidence level. PTX, paclitaxel; GEM, gemcitabine; SG, sulfated galactan; LSG low molecular weight SG; and LSGO, octanoyl ester-supplemented SG.

in cellular metabolism, surface receptor expression, and intracellular signaling between normal and cancer cells (37).

In the present study, these effects were achieved through the downregulation of upstream signaling molecules of PI3K/Akt/mTOR, ERK, and CDKs at both the gene and protein levels. This downregulation may be attributed to the structural similarity of SG derivatives to heparan sulfate proteoglycans (HSPGs), which can bind to growth factor receptors and/or ligands, thereby inhibiting receptor-ligand complex formation (13). It has been demonstrated that natural SPs share structural similarities with HSPGs and can mimic their functions. These SPs can interfere with the binding of growth factors to their receptors or co-receptors, leading to the inhibition of downstream signaling pathway activation in cancer cells (38). However, previous research indicates that SG derived from *G. fisheri* does not directly interact with EGF, but instead interacts with the EGFR, resulting in the downregulation of EGFR activity in CCA cells (14). The competitive binding of SG may disrupt receptor dimerization, leading to a reduction in p-EGFR and p-ERK levels (14). Therefore, by inhibiting growth factor receptors such as EGFR, SG derivatives may indirectly regulate PI3K/Akt/mTOR and ERK signaling molecules.

In MCF-7 cells treated with LSGO, the decreased expression of PI3K, AKT, mTOR and ERK at both the mRNA and protein levels resulted in a reduction of cyclin D1 and CDK4 expression, the first protein complex to become active in the G1 phase (39). The downregulation of cyclin D1 and CDK4 leads to the decreased transcription of key target genes, including cyclin E, cyclin B, CDK2 and CDK1, thereby disrupting cell cycle progression from the G1 to S phase (40). Furthermore, the downregulation of genes involved in the G1 and S phases also led to reduced expression of cyclin A and CDK2 at both the gene and protein levels. Given their critical roles in DNA synthesis, proper S phase progression, and the transition from S to G2 phase, this reduction may significantly affect cell cycle regulation (41). The findings of the present study indicate that SG derivatives, particularly LSGO induced cell cycle arrest at the G2/M phase in MCF-7 cells, potentially through the downregulation of cyclin/CDK complexes, particularly cyclin A and CDK2. These results are in contrast to those of previous studies reporting that SG derived from

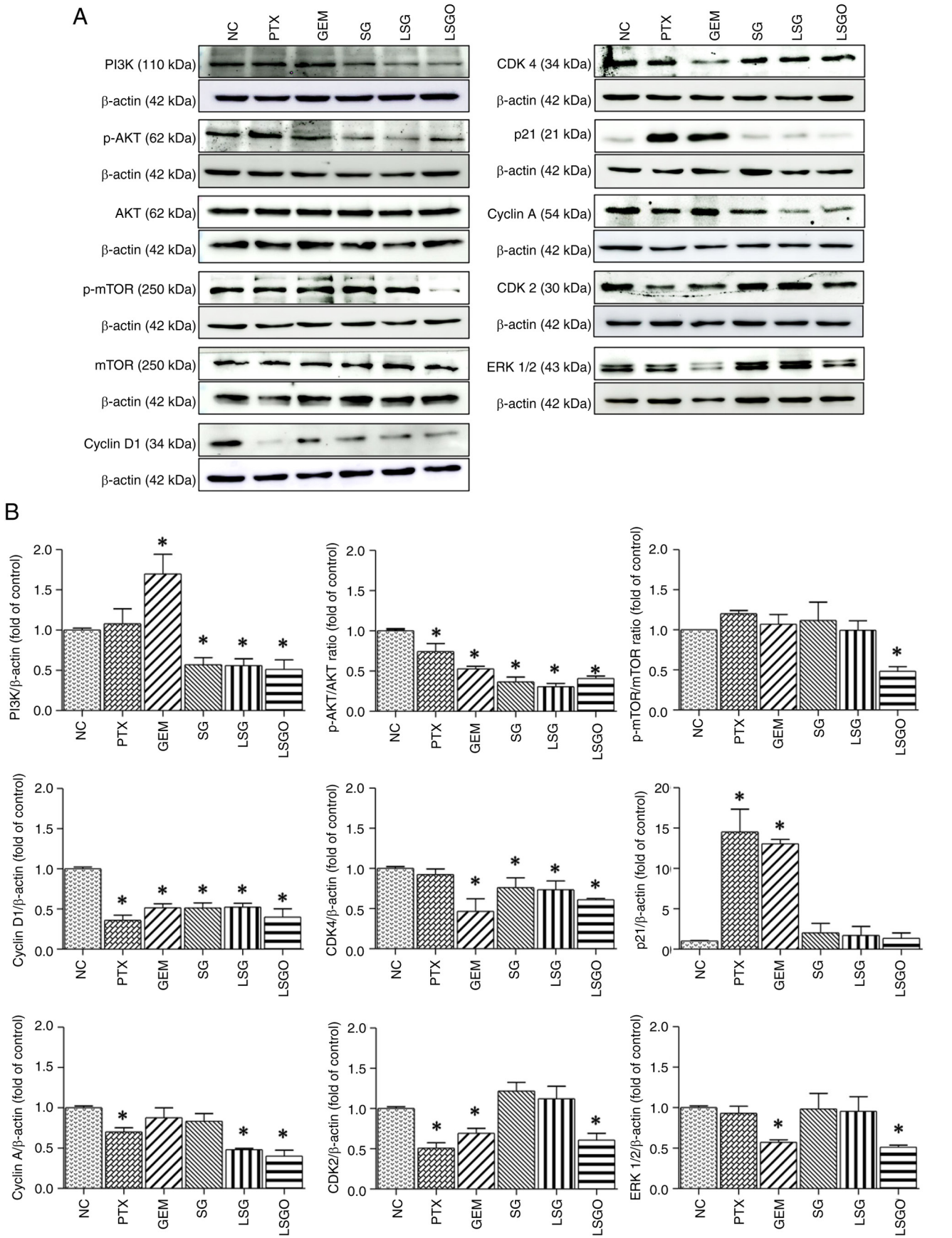

Figure 6. Effects of PTX, GEM, SG, LSG and LSGO on protein expression levels in MCF-7 cells, assessed using western blot analysis. (A) Protein expression levels of PI3K, p-AKT, AKT, p-mTOR, mTOR, cyclin D1, CDK4, p21, cyclin A, CDK2 and ERK 1/2 in MCF-7 cells treated with PTX, GEM, SG, LSG and LSGO, assessed using western blot analysis. (B) Quantitative analysis of PI3K, p-AKT/AKT, p-mTOR/mTOR, cyclin D1, CDK4, p21, cyclin A, CDK2 and ERK 1/2 expression, normalized to β-actin. The results are presented as the mean±SEM (n=3) from three independent experiments. *P<0.05, statistically significant difference compared to the normal control at a 95% confidence level. PTX, paclitaxel; GEM, gemcitabine; SG, sulfated galactan; LSG low molecular weight SG; and LSGO, octanoyl ester-supplemented SG.

G. fisheri induces cell cycle arrest at the G1 phase in CCA cells by downregulating cyclin D, cyclin E, CDK4 and CDK2. This reduction in cyclin/CDK expression is associated with the upregulation of p53 and p21, a key regulator of cyclin/CDK inhibition (13). By contrast, these findings suggest that the anti-proliferative effect of SG derivatives in MCF-7 cells is not mediated by the increased expression of p21.

Another possible explanation for why SG derivatives inhibit MCF-7 cell proliferation at the G2/M phase, including the reduction of cyclin A and CDK2, may be related to the structure-activity association of SG derivatives and cancer cell type specificity (26). Polysaccharides from different sources have been reported to induce cell cycle arrest at various phases in different cancer cell lines (35). For example, SP from *Laetiporus sulphureus* fruiting bodies has been shown to induce cell cycle arrest at the G0/G1 phase in triple-negative breast cancer MDA-MB-231 cells (42). Similarly, a homogeneous polysaccharide from *Crataegus* (Hawthorn) inhibited the proliferation of human colon cancer HCT116 cells by inducing cell cycle arrest at the S/G2 phase (35). Additionally, the combination of fucoidan with natural/organic ingredients, including vegetable juice, mulberry and wheatgrass, has been reported to increase the proportion of cells arrested in the G2/M phase in oral squamous cell carcinoma (43). The implications of the findings of the present study extend beyond breast cancer treatment, as the cell cycle regulatory proteins targeted by SG derivatives are involved in various cancer types. While previous studies have reported individual chemical modifications of SG, such as molecular weight reduction and esterification, the present study is the first to combine both modifications in a single structure. This combination resulted in the disruption of breast cancer cells and the inhibition of key signaling pathways in MCF-7 cells. These findings support the potential use of LSGO as an optimized SG derivative with enhanced anti-proliferative activity compared to either unmodified SG or SG with reduced molecular weight alone. Although the present study demonstrates the modulation of the PI3K/AKT and ERK signaling pathways following treatment with SG and its derivatives, further studies incorporating pathway-specific inhibitors or gene silencing approaches are warranted to validate the causal involvement of these pathways in mediating the observed anti-proliferative and cytotoxic effects. Additionally, future research is required to include Annexin V/PI staining to clarify the apoptosis-related mechanisms of SG and its derivatives, investigate their molecular interactions with regulatory proteins, evaluate their efficacy in *in vivo* models, and explore their potential synergy with existing chemotherapeutic agents to reduce side-effects in with breast cancer.

In conclusion, the results of the present study indicate that SG derivatives from *G. fisheri* exhibit mild, yet effective anti-proliferative activity in MCF-7 cells by inhibiting cell proliferation and inducing cell cycle arrest at the G2/M phase. This effect is mediated through the inhibition of upstream signaling molecules, cyclins and CDKs, which regulate MCF-7 cell proliferation. These findings highlight the potential use of SG derivatives, particularly LSGO, as natural compounds for breast cancer treatment and warrant further investigation into their clinical applications.

Acknowledgements

The authors would like to thank Dr Dylan Southard (the KKU Publication Clinic, Khon Kaen University, Khon Kaen, Thailand) for editing the manuscript.

Funding

The present study was supported by a Postgraduate Study Support Grant of the Faculty of Medicine, Khon Kaen University and the Faculty of Medicine, Khon Kaen University, Khon Kaen, Thailand (Grant no. IN66081).

Availability of data and materials

The data generated in the present study may be requested from the corresponding author.

Authors' contributions

JP and TR conceived and designed the study. JP, SS and TR performed the experiments. JP, SS, WS, TS, JK, KW and TR were responsible for data analysis. JP, SS and TR participated in the drafting of the manuscript. JK, KW and TR edited and finalized the manuscript. JK, KW and TR supervised the study. JP and TR provided funding and managed the project. JP, SS and TR confirm the authenticity of all the raw data. All authors have read and approved the final manuscript.

Ethics approval and consent to participate

Not applicable.

Patient consent for publication

Not applicable.

Competing interests

The authors declare that they have no competing interests.

References

1. Ilango S, Paital B, Jayachandran P, Padma PR and Nirmaladevi R: Epigenetic alterations in cancer. Front Biosci (Landmark Ed) 25: 1058-1109, 2020.
2. Damiescu R, Efferth T and Dawood M: Dysregulation of different modes of programmed cell death by epigenetic modifications and their role in cancer. Cancer Lett 584: 216623, 2024.
3. Feng Y, Spezia M, Huang S, Yuan C, Zeng Z, Zhang L, Ji X, Liu W, Huang B, Luo W, *et al*: Breast cancer development and progression: Risk factors, cancer stem cells, signaling pathways, genomics, and molecular pathogenesis. Genes Dis 5: 77-106, 2018.
4. Lee S, Rauch J and Kolch W: Targeting MAPK signaling in cancer: Mechanisms of drug resistance and sensitivity. Int J Mol Sci 21: 1102, 2020.
5. Dong C, Wu J, Chen Y, Nie J and Chen C: Activation of PI3K/AKT/mTOR pathway causes drug resistance in breast cancer. Front Pharmacol 12: 628690, 2021.
6. Mangé A, Coyaud E, Desmetz C, Laurent E, Béganton B, Coopman P, Raught B and Solassol J: FKBP4 connects mTORC2 and PI3K to activate the PDK1/Akt-dependent cell proliferation signaling in breast cancer. Theranostics 9: 7003-7015, 2019.
7. Palmer N and Kaldis P: Less-well known functions of cyclin/CDK complexes. Semin Cell Dev Biol 107: 54-62, 2020.

8. Ding L, Cao J, Lin W, Chen H, Xiong X, Ao H, Yu M, Lin J and Cui Q: The roles of cyclin-dependent kinases in cell-cycle progression and therapeutic strategies in human breast cancer. Int J Mol Sci 21: 1960, 2020.
9. Al Bitar S and Gali-Muhtasib H: The role of the cyclin dependent kinase inhibitor $p21^{cip1/waf1}$ in targeting cancer: Molecular mechanisms and novel therapeutics. Cancers (Basel) 11: 1475, 2019.
10. Menon SS, Guruvayoorappan C, Sakthivel KM and Rasmi RR: Ki-67 protein as a tumour proliferation marker. Clin Chim Acta 491: 39-45, 2019.
11. Burcombe R, Wilson GD, Dowsett M, Khan I, Richman PI, Daley F, Detre S and Makris A: Evaluation of Ki-67 proliferation and apoptotic index before, during and after neoadjuvant chemotherapy for primary breast cancer. Breast Cancer Res 8: R31, 2006.
12. Liyanage UE, Law MH, Han X, An J, Ong JS, Gharahkhani P, Gordon S, Neale RE, Olsen CM; 23andMe Research Team, *et al*: Combined analysis of keratinocyte cancers identifies novel genome-wide loci. Hum Mol Genet 28: 3148-3160, 2019.
13. Sae-Lao T, Tohtong R, Bates DO and Wongprasert K: Sulfated galactans from red seaweed Gracilaria fisheri target EGFR and inhibit cholangiocarcinoma cell proliferation. Am J Chin Med 45: 615-633, 2017.
14. Sae-Lao T, Luplertlop N, Janvilisri T, Tohtong R, Bates DO and Wongprasert K: Sulfated galactans from the red seaweed Gracilaria fisheri exerts anti-migration effect on cholangiocarcinoma cells. Phytomedicine 36: 59-67, 2017.
15. Fan J, Zhu J, Zhu H, Zhang Y and Xu H: Potential therapeutic target for polysaccharide inhibition of colon cancer progression. Front Med (Lausanne) 10: 1325491, 2024.
16. Rudtanatip T, Somintara S, Sakaew W, El-Abid J, Cano ME, Jongsomchai K, Wongprasert K and Kovensky J: Sulfated galactans from Gracilaria fisheri with supplementation of octanoyl promote wound healing activity in vitro and in vivo. Macromol Biosci 22: e2200172, 2022.
17. Srimongkol P, Songserm P, Kuptawach K, Puthong S, Sangtanoo P, Thitiprasert S, Thongchul N, Phunpruch S and Karnchanatat A: Sulfated polysaccharides derived from marine microalgae, Synechococcus sp. VDW, inhibit the human colon cancer cell line Caco-2 by promoting cell apoptosis via the JNK and p38 MAPK signaling pathway. Algal Res 69: 102919, 2023.
18. Aslama A, Bergerb MR, Ullaha I, Hameeda A and Masoodc F: Preparation and evaluation of cytotoxic potential of paclitaxel containing poly-3-hydroxybutyrate-co-3-hydroxyvalarate (PTX/PHBV) nanoparticles. Braz J Biol 83: e275688, 2023.
19. Dehghani N, Tafvizi F and Jafari P: Cell cycle arrest and anti-cancer potential of probiotic *Lactobacillus rhamnosus* against HT-29 cancer cells. Bioimpacts 11: 245-252, 2021.
20. Intuyod K, Hahnvajanawong C, Pinlaor P and Pinlaor S: Anti-parasitic drug ivermectin exhibits potent anticancer activity against gemcitabine-resistant cholangiocarcinoma in vitro. Anticancer Res 39: 4837-4843, 2019.
21. Livak KJ and Schmittgen TD: Analysis of relative gene expression data using real-time quantitative PCR and the 2(-Delta Delta C(T)) method. Methods 25: 402-408, 2001.
22. Shendge AK, Basu T and Mandal N: Evaluation of anticancer activity of *Clerodendrum viscosum* leaves against breast carcinoma. Indian J Pharmacol 53: 377-383, 2021.
23. Bray F, Laversanne M, Sung H, Ferlay J, Siegel RL, Soerjomataram I and Jemal A: Global cancer statistics 2022: GLOBOCAN estimates of incidence and mortality worldwide for 36 cancers in 185 countries. CA Cancer J Clin 74: 229-263, 2024.
24. Marquette C and Nabell L: Chemotherapy-resistant metastatic breast cancer. Curr Treat Options Oncol 13: 263-275, 2012.
25. He X, Xue M, Jiang S, Li W, Yu J and Xiang S: Fucoidan promotes apoptosis and inhibits EMT of breast cancer cells. Biol Phram Bull 42: 442-447, 2019.
26. Chantree P, Na-Bangchang K and Martviset P: Anticancer activity of fucoidan via apoptosis and cell cycle arrest on cholangiocarcinoma cell. Asian Pac J Cancer Prev 22: 209-217, 2021.
27. Wongprasert K, Rudtanatip T and Praiboon J: Immunostimulatory activity of sulfated galactans isolated from the red seaweed Gracilaria fisheri and development of resistance against white spot syndrome virus (WSSV) in shrimp. Fish Shellfish Immunol 36: 52-60, 2014.
28. Li N, Wang C, Georgiev MI, Bajpai VK, Tundis R, Simal-Gandara J, Lu X, Xiao J, Tang X and Qiao X: Advances in dietary polysaccharides as anticancer agents: Structure-activity relationship. Trends Food Sci Technol 111: 360-377, 2021.
29. Lu J, Shi KK, Chen S, Wang J, Hassouna A, White LN, Merien F, Xie M, Kong Q, Li J, *et al*: Fucoidan extracted from the New Zealand *Undaria pinnatifida*-physicochemical comparison against five other fucoidans: Unique low molecular weight fraction bioactivity in breast cancer cell lines. Mar Drugs 16: 461, 2018.
30. Wang Y, Xing M, Cao Q, Ji A, Liang H and Song S: Biological activities of fucoidan and the factors mediating its therapeutic effects: A review of recent studies. Mar Drugs 17: 183, 2019.
31. Sakaew W, Somintara S, Jongsomchai K, El Abid J, Wongprasert K, Kovensky J and Rudtanatip T: Octanoyl esterification of low molecular weight sulfated galactan enhances the cellular uptake and collagen expression in fibroblast cells. Biomed Rep 19: 99, 2023.
32. Davey MG, Hynes SO, Kerin MJ, Miller N and Lowery AJ: Ki-67 as a prognostic biomarker in invasive breast cancer. Cancers (Basel) 13: 4455, 2021.
33. Yang C, Zhang J, Ding M, Xu K, Li L, Mao L and Zheng J: Ki67 targeted strategies for cancer therapy. Clin Transl Oncol 20: 570-575, 2018.
34. Li LT, Jiang G, Chen Q and Zheng JN: Ki67 is a promising molecular target in the diagnosis of cancer (review). Mol Med Rep 11: 1566-1572, 2015.
35. Ma L, Xu GB, Tang X, Zhang C, Zhao W, Wang J and Chen H: Anti-cancer potential of polysaccharide extracted from hawthorn (Crataegus.) on human colon cancer cell line HCT116 via cell cycle arrest and apoptosis. J Funct Foods 64: 103677, 2020.
36. Abdala-Díaz RT, Casas-Arrojo V, Castro-Varela P, Riquelme C, Carrillo P, Medina MA, Cárdenas C, Becerra J and Pérez Manríquez C: Immunomodulatory, antioxidant, and potential anticancer activity of the polysaccharides of the fungus *Fomitiporia chilensis*. Molecules 29: 3628, 2024.
37. Akhtar MJ, Ahamed M, Alhadlaq HA, Alrokayan SA and Kumar S: Targeted anticancer therapy: Overexpressed receptors and nanotechnology. Clin Chim Acta 436: 78-92, 2014.
38. Cheng JJ, Chang CC, Chao CH and Lu MK: Characterization of fungal sulfated polysaccharides and their synergistic anticancer effects with doxorubicin. Carbohydr Polym 90: 134-139, 2012.
39. Asghar U, Witkiewicz AK, Turner NC and Knudsen ES: The history and future of targeting cyclin-dependent kinases in cancer therapy. Nat Rev Drug Discov 14: 130-146, 2015.
40. Finn RS, Aleshin A and Slamon DJ: Targeting the cyclin-dependent kinases (CDK) 4/6 in estrogen receptor-positive breast cancers. Breast Cancer Res 18: 17, 2016.
41. Gopinathan L, Tan SL, Padmakumar VC, Coppola V, Tessarollo L and Kaldis P: Loss of Cdk2 and cyclin A2 impairs cell proliferation and tumorigenesis. Cancer Res 74: 3870-3879, 2014.
42. Jen CI, Lu MK, Lai MN and Ng LT: Sulfated polysaccharides of Laetiporus sulphureus fruiting bodies exhibit anti-breast cancer activity through cell cycle arrest, apoptosis induction, and inhibiting cell migration. J Ethnopharmacol 321: 117546, 2024.
43. Chen PH, Chiang PC, Lo WC, Su CW, Wu CY, Chan CH, Wu YC, Cheng HC, Deng WP, Lin HK and Peng BY: A novel fucoidan complex-based functional beverage attenuates oral cancer through inducing apoptosis, G2/M cell cycle arrest and retarding cell migration/invasion. J Funct Foods 85: 104665, 2021.